UNDOPED DIAMOND FILMS FOR TRANSDUCER APPLICATIONS

Lidia MOSIŃSKA[1], Paweł POPIELARSKI[1], Robert SZCZĘSNY[2], Agnieszka WIĘCKOWSKA[3], Michal KOČÍ[4], Kateřina AUBRECHTOVÁ DRAGOUNOVÁ[4], Rajisa JACKIVOVÁ[4]

[1]*Institute of Physics, Kazimierz Wielki University in Bydgoszcz, Powstańców Wielkopolskich Str. 2, Bydgoszcz, Poland, EU, lidiamosinska@ukw.edu.pl*

[2]*Faculty of Chemistry, Nicolaus Copernicus University in Torun, Gagarina 7, Torun, Poland, EU*

[3]*Department of Inorganic and Analytical Chemistry, Faculty of Chemistry, University of Warsaw, Pasteura 1 st., Warsaw, Poland, EU*

[4]*Institute of Physics of the Czech Academy of Sciences, Cukrovarnická 10, Prague, Czech Republic, EU*

https://doi.org/10.37904/nanocon.2025.5193

Abstract

Undoped diamond films were synthesized by Hot-Filament Chemical Vapor Deposition (HF-CVD) using gas mixtures containing 5–7 vol.% methanol in hydrogen. The influence of methanol concentration on film morphology, crystallinity and sensing performance was systematically investigated. SEM and XRD analyses confirmed the formation of polycrystalline diamond layers with grain sizes of 13–24 nm, while Raman spectra revealed the characteristic diamond peak near 1332 cm^{-1} and a controlled contribution of sp^2-bonded carbon. The electrical behavior of the films depended on the sp^2 fraction, enabling tunable conductivity without intentional doping. Electrochemical tests demonstrated that the obtained undoped films exhibit stable and monotonic responses to pH and CO_2, indicating their suitability for transducer applications. The results show that appropriate optimization of HF-CVD growth conditions allows fabrication of functional diamond sensing layers without the need for boron doping, simplifying processing while maintaining favorable electrical and chemical properties.

Keywords: Undoped diamond films, HF-CVD, sensor materials, transducer applications

1. INTRODUCTION

Diamond thin films are widely recognised as advanced materials for sensing and transducer applications due to their exceptional chemical stability, extreme hardness, wide band gap and high thermal conductivity [1, 2]. Their broad electrochemical potential window and low background currents make them attractive for use in harsh chemical environments, biomedical interfaces and microelectronic systems [3, 4]. While most electrochemical studies have traditionally focused on boron-doped diamond (BDD) because of its high conductivity [5, 6], numerous reports have demonstrated that undoped CVD diamond may also exhibit semiconducting behaviour arising from grain-boundary states, sp^2-rich regions and hydrogen-terminated surfaces [7, 8].

Early work by Pleskov et al. showed that undoped CVD diamond can act as a functional semiconductor electrode governed by defect-related acceptor states [9, 10]. Further studies confirmed that film morphology, crystallite size and the sp^2/sp^3 ratio strongly influence charge transport and electrochemical activity in undoped polycrystalline diamond [11, 12]. In particular, hydrogen termination induces a p-type surface conductive layer, allowing nominally insulating diamond to participate in charge-transfer processes relevant to pH sensing and solution-gated FET devices [13, 14].

Among CVD techniques, Hot Filament CVD (HF-CVD) offers a cost-effective and scalable method for producing uniform polycrystalline diamond films on various substrates [15, 16]. Growth conditions—including hydrocarbon concentration, pressure and substrate temperature—directly determine structural quality, grain size and the presence of non-diamond carbon, all of which affect electrical and electrochemical properties [17, 18]. Recent studies have shown that carefully engineered undoped HF-CVD diamond films can combine a wide potential window with sufficiently high conductivity and stable interfacial kinetics, enabling their use in chemical and electrochemical transducers [19, 20].

The present work investigates undoped HF-CVD diamond films with the aim of correlating growth parameters with structural and electrochemical characteristics relevant to transducer applications [20]. By analysing morphology, Raman spectra and sensing performance, we demonstrate that undoped diamond—without intentional doping—can serve as an effective and reproducible material for pH and gas-sensitive transducers.

2. MATERIALS AND METHODS

2.1. Deposition of undoped diamond films

Undoped diamond films were synthesized using a Hot Filament Chemical Vapor Deposition (HF-CVD) system equipped with tungsten filaments. The HF-CVD reactor used in this study is schematically shown in **Figure 1**.

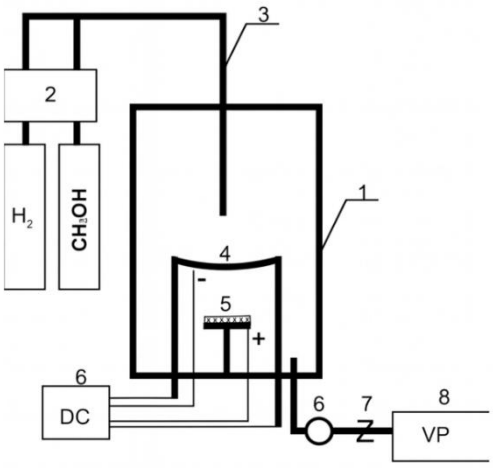

where:

(1) inside the reactor
(2) mass flowmeters
(3) mixture of hydrogen and hydrocarbon
(5) substrate holder
(6) DC power supply
(7) needle valve

Figure 1 Scheme of HF CVD reactor

Silicon substrates were ultrasonically cleaned, seeded with nanodiamond suspension, and mounted at a fixed distance from the filament. The gas mixture consisted of hydrogen and methanol vapour, with methanol concentration varied between 4–7%. The total gas flow was kept at 100 sccm, the chamber pressure at 50 mbar, and the substrate temperature at approximately 1000 K. All depositions were carried out for 6 hours. The selected process window allowed controlled variation of grain size and sp^2/sp^3 ratio, enabling correlation of growth conditions with film performance.

2.2. Structural and morphological characterization

Film morphology and thickness were examined using Scanning Electron Microscopy (SEM). Raman spectroscopy (λ = 442 nm) was employed to evaluate the structural quality of the films, including crystallite size effects and the relative contributions of sp^2- and sp^3-bonded carbon. Particular attention was given to the analysis of the D band (~1379 cm^{-1}) and G band (~1603 cm^{-1}), whose positions, widths and intensity ratios provide insight into the degree of disorder and the sp^2 fraction within the films. X-ray diffraction (XRD)

measurements (Cu Kα radiation, 2θ range 30–90°) were performed to identify the crystalline phases present and to assess preferential orientation through the evaluation of diamond (111), (220) and (311) reflections.

2.3. Electrical measurements

Electrical transport was examined using temperature-dependent I–V measurements, enabling identification of dominant conduction mechanisms (grain-boundary transport, hopping processes, surface conductivity). The sensing performance was tested toward pH variations and selected gases (e.g., CO_2) to determine the films' suitability for transducer applications.

3. RESULTS AND DISCUSSION

3.1. Morphology and microstructure

SEM analysis revealed that all deposited films formed continuous, well-adhered layers exhibiting a nanocrystalline morphology. The grain size varied systematically with methanol concentration: films grown at 7% MeOH contained crystallites of approximately 13–15 nm, whereas those deposited at 5% MeOH exhibited larger grains in the range of 20–24 nm. The samples produced at intermediate MeOH concentrations showed grain sizes between these two limits. Representative SEM images of the films grown at 5–7% MeOH are presented in **Figure 2**.

An increase in the hydrocarbon (MeOH) content resulted in enhanced secondary nucleation, which manifested as a higher density of grain boundaries and the formation of smaller, less uniformly shaped crystallites. These morphological trends are consistent with typical HF-CVD growth behaviour, where the carbon precursor concentration strongly influences both the nucleation rate and the balance between vertical and lateral grain growth.

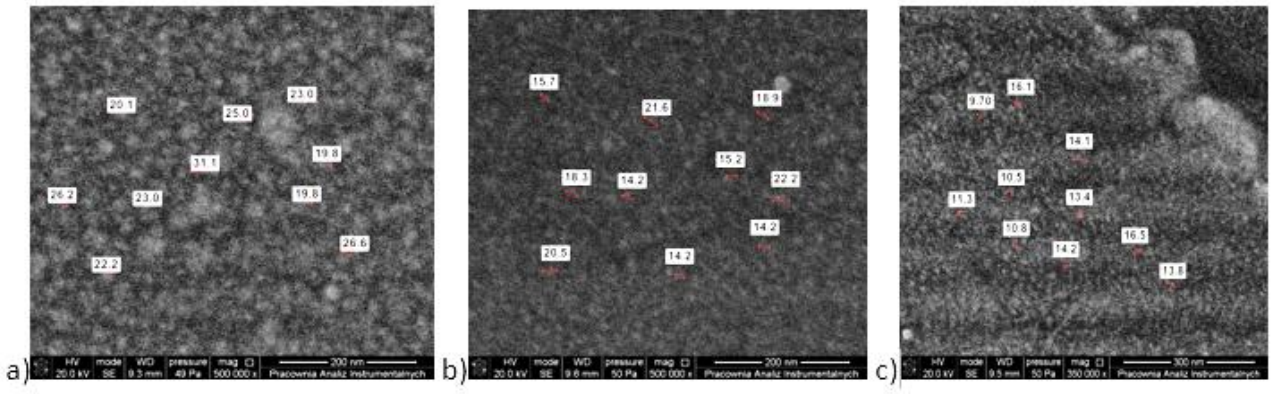

Figure 2 CVD diamond films, with the content of the vapors of methanol in quantity: a) 5% CH_3OH, b) 6% CH_3OH, c) 7% CH_3OH

Raman spectra of the deposited films exhibit features typical for nanocrystalline diamond layers containing a controlled amount of non-diamond carbon. The characteristic diamond line at ~1332 cm^{-1}, associated with sp^3-bonded carbon, is not clearly visible due to the small grain size and significant contribution of disordered carbon phases. Instead, the spectra are dominated by two broad bands located at 1379 cm^{-1} and 1603 cm^{-1}, which correspond to the D band (breathing modes of sp^2 ring structures) and the G band (E2g stretching mode of sp^2-bonded carbon), respectively.

The relative intensities and widths of these two bands indicate differences in the fraction and disorder of sp^2 carbon as a function of methanol concentration during growth. An increase in the G-band intensity and its

upshift toward ~1600 cm^{-1} typically reflects a higher amount of graphitic or amorphous sp^2 carbon and increased structural disorder. **Figure 3** summarises the Raman spectra of the films deposited at different MeOH concentrations. This behavior is consistent with the small grain sizes observed in SEM and with XRD peak broadening.

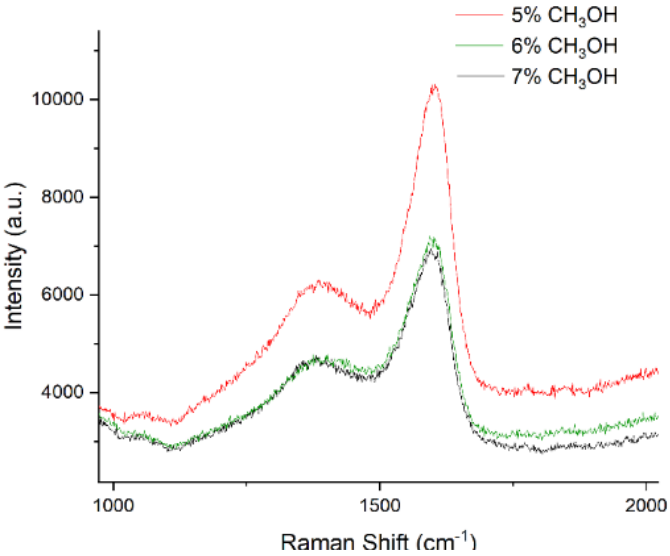

Figure 3 Raman spectra of the layers grown at concentration of methanol ranged from 5% to 7% CH_3OH

Because sp^2-rich grain boundaries facilitate charge transport, the variation in the D/G ratio provides qualitative insight into electrical properties discussed later. Films exhibiting a slightly higher sp^2 contribution (e.g., at higher MeOH content) show increased conductivity, which supports their performance in sensing applications.

Quantitative Raman analysis was performed by evaluating the ID/IG peak intensity ratio after signal normalization. The calculated ID/IG values were 0.59, 0.64 and 0.70 for the films grown at 5%, 6% and 7% MeOH, respectively. This confirms the increase of the sp^2 carbon content with rising MeOH concentration, which correlates well with the observed reduction in grain size (**Figure 2**) and the enhanced charge transport pathways reflected in the sensing performance (Section 3.2).

The XRD patterns of the films synthesised with 5%, 6% and 7% MeOH confirm the formation of polycrystalline diamond, as evidenced by the presence of the (111), (220) and (311) reflections typical of the cubic diamond structure. However, clear differences in peak intensities and widths are observed across the series. The film deposited at 5% MeOH shows the sharpest and most intense (111) reflection, which is characteristic of larger coherent scattering domains and a lower degree of lattice disorder. For the film grown at 6% MeOH, the diffraction peaks become slightly broader and their intensities decrease, indicating a reduction in crystallite size. For the film grown at 7% MeOH, the (111) reflection becomes even broader and less intense, confirming the trend towards smaller crystallites and increased structural disorder. The corresponding XRD spectra are shown in **Figure 4**.

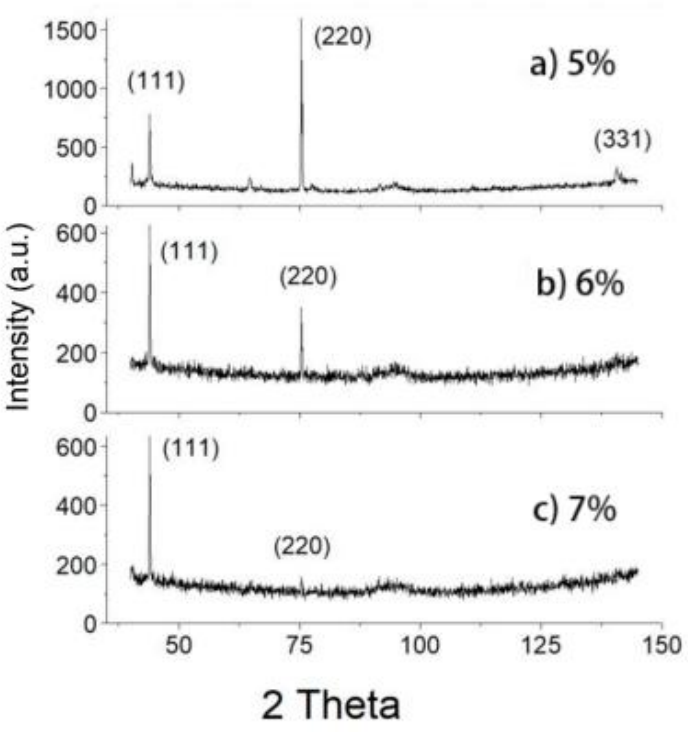

Figure 4 Diffraction spectra for: a) 5% CH_3OH , b) 6% CH_3OH, c) 7% CH_3OH

3.2. Sensing performance

The sensing behaviour of the undoped diamond films was evaluated by recording their current–voltage (I-V) characteristics under exposure to CO_2 and to aqueous environments of different pH. The results are presented in **Figure 5**. Although the measurements do not directly yield conductance values, the systematic modulation of the I-V characteristics provides clear evidence of transduction capability.

For the film grown at 5% MeOH, exposure to CO_2 at flow rates of 10, 50 and 90 ml/h resulted in distinct and reproducible shifts in the I-Vcurves (**Figure 5a**). The curves gradually separate as the CO_2 flow increases, indicating that the electrical response of the layer is sensitive to changes in gas composition. This behaviour demonstrates that even undoped nanocrystalline diamond films can transduce gas-phase perturbations into an electrical signal through modifications of the charge-transport pathways.

A similarly pronounced effect was observed in liquid-phase measurements performed on the film deposited at 7% MeOH. As shown in **Figure 5b**, the I-V curves recorded in buffer solutions of pH 4, 7 and 9 exhibit systematic shifts, particularly at negative polarisation. Higher pH values correspond to characteristic curve displacements, allowing clear differentiation between the tested environments. This response reflects the sensitivity of the film's surface states and grain-boundary network to pH-dependent changes in interfacial charge.

Both CO_2-and pH-dependent measurements exhibit clear and reproducible current shifts at +1.0 V, confirming effective transduction behaviour. As shown in **Figure 5a**, the 5% MeOH film responds to the increasing CO_2 flow with a current change of ~0.60 nA (10-90 ml/h), whereas the 7% MeOH film reveals a stronger modulation for pH variations (~0.70 nA between pH 4 and 9), as presented in **Figure 5b**. This difference reflects that pH changes directly modulate the surface charge and electrical conductivity along the grain-boundary network. The results demonstrate that the microstructure, governed by methanol content during growth, enables functional sensing without intentional doping.

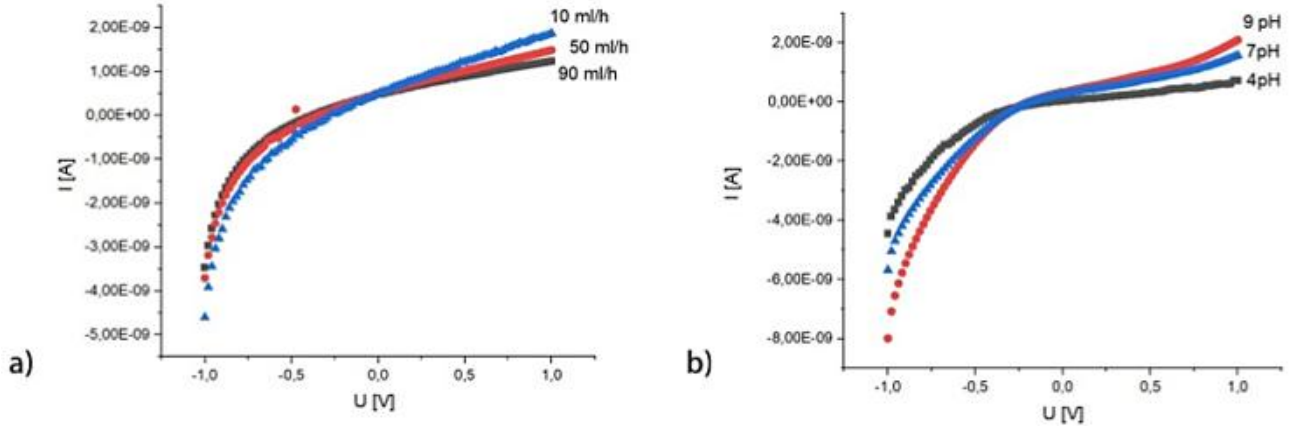

Figure 5 Current–voltage (I--V) characteristics of undoped HF-CVD diamond films used as transducers: (a) response of the film grown at 5% MeOH to CO_2 flow rates of 10, 50 and 90 ml/h; (b) response of the film grown at 7% MeOH in buffer solutions of pH 4, 7 and 9.

4. CONCLUSION

Undoped diamond films were successfully synthesised by HF-CVD, and controlled variation of the methanol concentration enabled systematic tuning of their microstructure and sp^2 content. SEM, Raman and XRD analyses confirmed that higher MeOH levels promote smaller crystallites, increased grain-boundary density and a higher share of disordered carbon.

The films demonstrated stable and monotonic electrical responses to CO_2 and pH variations, evidenced by systematic shifts of the I-V characteristics. This confirms that undoped nanocrystalline diamond can operate effectively as a transducer material without the need for intentional doping.

Overall, the results show that optimisation of HF-CVD growth parameters provides a simple and scalable route to functional diamond sensing layers, offering a promising alternative to doped diamond electrodes for chemical and electrochemical transducer applications.

ACKNOWLEDGEMENTS

The work was performed in the frame of MNSW Poland Regional Excellence Initiative no. RID/SP/0048/2024/01 project.

REFERENCES

[1] CLAUSING, R.E., et al. Diamond and diamond-like films and coatings. *Springer Science & Business Media*. 2012

[2] SRIKANTH, V. Review of advances in diamond thin film synthesis, *Proceedings of the Institution of Mechanical Engineers, Part C: Journal of Mechanical Engineering Science*. 2012

[3] SWAIN, G.M., A.B. ANDERSON, and J.C. ANGUS, Applications of diamond thin films in electrochemistry, *Mrs Bulletin*. 1998

[4] OBAID, S.N., Z. CHEN, and L. LU. Advanced electrical and optical microsystems for biointerfacing, *Advanced Intelligent Systems*. 2020

[5] EINAGA, Y. Diamond electrodes for electrochemical analysis, *Journal of applied electrochemistry*. 2010

[6] PANIZZA, M., E. BRILLAS, and C. COMNINELLIS. Application of boron-doped diamond electrodes for wastewater treatment, *J. Environ. Eng. Manag*. 2008

[7] ZHAO, F., et al. A review of diamond materials and applications in power semiconductor devices. *Materials*. 2024

[8] MOSINSKA, L., et al. Effect of sp (2) phase content on hydrophobicity of diamond layers, *Przemysl Chemiczny*, 2014

[9] PLESKOV, Y.V., et al. Photoelectrochemical properties of semiconductor diamond, *Journal of electroanalytical chemistry and interfacial electrochemistry*. 1987

[10] BHATTACHARYA, G., et al. Probing the flat band potential and effective electronic carrier density in vertically aligned nitrogen doped diamond nanorods via electrochemical method. *Electrochimica Acta*. 2017

[11] STUCHLIKOVÁ, T., et al. Electrical and optical characteristics of boron doped nanocrystalline diamond films. *Vacuum*. 2019

[12] MARTIN, H.B., et al. Voltammetry studies of single-crystal and polycrystalline diamond electrodes. *Journal of the Electrochemical Society*. 1999

[13] GEIS, M.W., et al. Progress toward diamond power field-effect transistors, *Physica status solidi (a)*, 2018

[14] SOHN, I.-Y., et al. pH sensing characteristics and biosensing application of solution-gated reduced graphene oxide field-effect transistors. *Biosensors and Bioelectronics*. 2013

[15] FUENTES-FERNANDEZ, E., et al. Synthesis and characterization of microcrystalline diamond to ultrananocrystalline diamond films via Hot Filament Chemical Vapor Deposition for scaling to large area applications. *Thin Solid Films*. 2016

[16] GUO, L. and G. CHEN. High-quality diamond film deposition on a titanium substrate using the hot-filament chemical vapor deposition method. *Diamond and related materials*. 2007

[17] BALMER, R., et al. Chemical vapour deposition synthetic diamond: materials, technology and applications. *Journal of Physics: Condensed Matter*. 2009

[18] YANG, N., et al. Conductive diamond: synthesis, properties, and electrochemical applications, *Chemical Society Reviews*. 2019

[19] YANG, N. and X. JIANG, Rational design of diamond electrodes, *Accounts of Chemical Research*. 2022

[20] MOSIŃSKA, L., et al. Diament jako materiał przetwornikowy do produkcji biosensorów. *Przemysł Chemiczny*. 2013